Published OnlineFirst March 1, 2011; DOI: 10.1158/1078-0432.CCR-10-1950

Cancer Therapy: Preclinical

Clinical Cancer Research

Nonproteasomal Targets of the Proteasome Inhibitors Bortezomib and Carfilzomib: a Link to Clinical Adverse Events

Shirin Arastu-Kapur[1], Janet L. Anderl[2], Marianne Kraus[3], Francesco Parlati[1], Kevin D. Shenk[1], Susan J. Lee[1], Tony Muchamuel[1], Mark K. Bennett[1], Christoph Driessen[3], Andrew J. Ball[2], and Christopher J. Kirk[1]

Abstract

Purpose: Bortezomib (Velcade), a dipeptide boronate 20S proteasome inhibitor and an approved treatment option for multiple myeloma, is associated with a treatment-emergent, painful peripheral neuropathy (PN) in more than 30% of patients. Carfilzomib, a tetrapeptide epoxyketone proteasome inhibitor, currently in clinical investigation in myeloma, is associated with low rates of PN. We sought to determine whether PN represents a target-mediated adverse drug reaction (ADR).

Experimental Design: Neurodegenerative effects of proteasome inhibitors were assessed in an *in vitro* model utilizing a differentiated neuronal cell line. Secondary targets of both inhibitors were identified by a multifaceted approach involving candidate screening, profiling with an activity-based probe, and database mining. Secondary target activity was measured in rats and patients receiving both inhibitors.

Results: Despite equivalent levels of proteasome inhibition, only bortezomib reduced neurite length, suggesting a nonproteasomal mechanism. In cell lysates, bortezomib, but not carfilzomib, significantly inhibited the serine proteases cathepsin G (CatG), cathepsin A, chymase, dipeptidyl peptidase II, and HtrA2/Omi at potencies near or equivalent to that for the proteasome. Inhibition of CatG was detected in splenocytes of rats receiving bortezomib and in peripheral blood mononuclear cells derived from bortezomib-treated patients. Levels of HtrA2/Omi, which is known to be involved in neuronal survival, were upregulated in neuronal cells exposed to both proteasome inhibitors but was inhibited only by bortezomib exposure.

Conclusion: These data show that bortezomib-induced neurodegeneration *in vitro* occurs via a proteasome-independent mechanism and that bortezomib inhibits several nonproteasomal targets *in vitro* and *in vivo*, which may play a role in its clinical ADR profile. *Clin Cancer Res; 17(9); 2734–43. ©2011 AACR.*

Introduction

Polypharmacology is the study of identifying secondary targets for an active pharmaceutical agent (drug promiscuity). In some disease etiologies, targeting multiple proteins may improve the therapeutic efficacy, such as for antipsychotic drugs or kinase inhibitors with anticancer activity (1). However, off-target activity can lead to adverse drug reactions (ADR) such as the case with fenfluramine and torcetrapib, 2 agents halted in development because of fatal hypertension that was the consequence of secondary target inhibition (1–3). Highlighting the promiscuity of small molecule inhibitors, a recent *in silico* screening of 213 Roche compounds revealed an average of 6.3 target proteins per compound (1). The standard approach for detecting off-target activity consists of screening compounds against panels of targets, often involving recombinant proteins in cell-free systems, and *in silico* prediction tools (1, 4). More recently, whole genome- and proteome-based analyses have been utilized to infer potential off-target activity, but these methods identify affected pathways rather than direct protein targets for a drug (3).

Bortezomib (Velcade) is a dipeptide boronate proteasome inhibitor that has been approved for the treatment of multiple myeloma (MM) and mantle cell lymphoma (5). The proteasome is a multicatalytic protease whose active sites are unique N-terminal threonine proteases (6, 7). Proteasome inhibition results in the modulation of many cellular activities, including alterations in signal transduction pathways, modifications in antigen presentation, and induction of an apoptotic response (5). Despite robust

Authors' Affiliations: [1]Research, Onyx Pharmaceuticals, Inc. South San Francisco, California, Onyx Pharmaceuticals, Inc., Emeryville, California; [2]Bioscience Division, Millipore Corporation, St. Charles, Missouri; and [3]Experimental Oncology and Clinical Trials Unit, Kantonsspital, St. Gallen, Switzerland

Note: Supplementary data for this article are available at Clinical Cancer Research Online (http://clincancerres.aacrjournals.org/).

Corresponding Author: Christopher J. Kirk, Research, Onyx Pharmaceuticals, Inc., 249 E. Grand Ave., South San Francisco, CA 94080. Phone: 650-266-2660; Fax: 866-778-9068. E-mail: ckirk@onyx-pharm.com

doi: 10.1158/1078-0432.CCR-10-1950

Published OnlineFirst March 1, 2011; DOI: 10.1158/1078-0432.CCR-10-1950

Translational Research

Bortezomib has validated the proteasome as a target for the treatment of myeloma but is hindered by a painful peripheral neuropathy (PN) that may occur because of proteasome inhibition. Carfilzomib, a second in class proteasome inhibitor, is in late-stage clinical trials and displays minimal signs of PN. These observations suggest a proteasome-independent mechanism (off-target activity) underlying PN.

In this study, we utilized an *in vitro* model of neurodegeneration in which, despite equivalent proteasome inhibition, only bortezomib induced neurite degeneration. Utilizing a multifaceted approach to identify off-targets that included activity-based probe (ABP) profiling in cells and *in silico* database mining, we found that bortezomib targets several serine hydrolases. We report the first demonstration of inhibition of a nonproteasomal target (cathepsin G) in bortezomib-treated patients using ABPs. Also, bortezomib inhibits a prosurvival protease, HtrA2/Omi, in neuronal cells, supporting the hypothesis that bortezomib-induced PN results from off-target activity.

antitumor activity in the clinic, bortezomib therapy is hindered by a treatment-emergent peripheral neuropathy (PN). In relapsed and/or refractory MM, single-agent bortezomib results in PN in 35% to 52% of patients with grade 3/4 rates ranging from 8% to 14% (8–11). The mechanism of this neuropathy is unknown but may represent the effects of proteasome inhibition in sensory neurons (12).

The clinical success of bortezomib has led to the development of several new proteasome inhibitors, including agents with chemical structures distinct from bortezomib (13, 14). Of these, carfilzomib, a tetrapeptide epoxyketone, is the furthest in clinical development, with phase 2 trials in myeloma and solid tumors ongoing (15). Recently, it was reported that treatment-emergent neuropathy occurred in 14.6% of 505 treated patients, with 1.2% reaching a grade 3/4 level (16, 17). Carfilzomib and bortezomib display an equivalent potency for the chymotrypsin-like (CT-L) subunits of the proteasome but differ in the length of their peptide backbone (tetrapeptide vs. dipeptide) and in the reactive pharmacophore responsible for inhibition of proteasome active sites (13, 14, 18). The epoxyketone warhead of carfilzomib forms a dual covalent adduct that can be formed only with the side-chain hydroxyl and free amine of the N-terminal threonine active site that is found exclusively within the proteasome. On the other hand, the boronate warhead of bortezomib forms a tetrahedral intermediate with the side-chain hydroxyl group (13). This tetrahedral intermediate can also be formed with other classes of proteases, such as serine proteases. Indeed, cathepsin G (CatG) and chymase, 2 serine proteases, were previously shown to be targets of bortezomib, but their inhibition in enzymatic assays using purified enzymes was reported to occur at concentrations 100-fold or more above that required for proteasome inhibition (19). However, the activity of bortezomib against nonproteasomal proteases in physiologic conditions (i.e., in cells or *in vivo*) has not been determined and the contribution of on- and off-target effects in the induction of PN remains an open question.

We report here that bortezomib induces neurotoxicity by a proteasome-independent mechanism in an *in vitro* model of neurodegeneration, which involves the quantitation of neurite length and cell survival in differentiated SH-SY5Y (neuroblastoma) cells. To investigate the propensity of bortezomib and carfilzomib to inhibit nonproteasomal targets, we pursued a multifaceted approach utilizing a panel of purified enzymes, activity-based probe (ABP) profiling in cells and cell lysates, and *in silico* database mining. The results presented here are the first practical application of ABPs for profiling off-target activity of an Food and Drug Administration–approved drug. Using both purified enzymes and ABP, we were able to show that bortezomib targets several serine hydrolases, including CatG, cathepsin A (CatA), chymase, and dipeptidyl peptidase II (DPPII). By the ABP approach, which enabled the measurement of activity in cells and *in vivo*, we found that the potency of bortezomib against several serine proteases was higher than previously reported. Furthermore, we have shown inhibition of CatG in splenocytes from bortezomib-treated rats and in peripheral blood mononuclear cells (PBMC) from bortezomib-treated patients. Finally, through both database mining and substrate monitoring in SH-SY5Y cells, we found that bortezomib is a potent inhibitor of HtrA2/Omi, a stress-induced protease involved in neuronal cell survival. Interestingly, carfilzomib showed almost no inhibitory activity against serine proteases *in vitro* and *in vivo*. Taken together, these data support the hypothesis that PN is not a class effect of proteasome inhibitors and may involve off-target inhibition by bortezomib.

Methods

Compounds

The biotinylated general serine hydrolase flurophosphonate-biotin (FP-biotin) probe was synthesized as previously described (20). Bortezomib (Fig. 1A) was purchased from a pharmacy. Cbz-Leu-Leu-Leu-boronic acid was purchased from AG Scientific, Inc. MG-132 (Cbz-Leu-Leu-Leu-aldehyde) was purchased from Boston Biochem.

Carfilzomib (Fig. 1A) was synthesized as previously described (US 07232818). Cbz-Leu-Phe-ketoepoxide and Cbz-Leu-Leu-Leu-ketoepoxide were synthesized as previously described (WO 2005111008) with more than 95% purity by high-performance liquid chromatography (HPLC) and nuclear magnetic resonance (NMR) methods. Cbz-Leu-Phe-aldehyde was synthesized as previously described (21), and the aldehyde version of carfilzomib was synthesized by the reduction of the Weinreb amide of carfilzomib to an aldehyde with lithium aluminum hydride in tetrahydrofuran with more than 75% purity by HPLC and NMR methods.

Published OnlineFirst March 1, 2011; DOI: 10.1158/1078-0432.CCR-10-1950

Cells

PBMCs from normal healthy volunteers were obtained from AllCells. HepG2 (hepatocellular carcinoma), THP-1 (acute monocytic leukemia), 786-O (renal cell adenocarcinoma), and SH-SY5Y (neuroblastoma) cells were obtained from the American Type Culture Collection and were cultured in media recommended by the supplier at 37°C in 5% CO_2.

Animals

Male Sprague-Dawley rats (275–300 g) were purchased from Charles River Laboratories and housed for 1 week before experimentation. For all experiments, animals had access to food and water *ad libitum*. All experiments were done under protocols approved by an institutional animal care and use committee.

SH-SY5Y neurodegeneration assay

This assay was conducted as previously described (22, 23). Briefly, SH-SY5Y cells were differentiated in multiwell plates by culturing in the presence of retinoic acid for 5 days, followed by exposure to brain-derived neurotrophic factor for 3 days. The cells were then treated with compound for 24, 48, and/or 72 hours, fixed, and stained with Hoechst (blue) for identification of cell nuclei staining to identify live cells and neuronal-specific βIII-tubulin (green) for the cytoskeleton to visualize cell bodies and neurites. Endpoint analysis was done by high-content imaging and quantitative image analysis on an IN Cell Analyzer 1000 system (GE Healthcare), utilizing software designed to segment cellular morphologic features based on size- and fluorescence intensity–related criteria.

Purified enzyme assays

Substrate-based assays were initiated by enzyme addition and monitored for aminoacyl 7-amino-4-methylcoumarin amide (MCA) and 7-amino-4-methylcoumarin (AMC) product formation with a plate-based spectrofluorometer (Tecan). Chymase (EMD Chemicals) activity was measured using Suc-Ala-Ala-Pro-Phe-AMC (MP Biomedicals) in assay buffer consisting of 200 mmol/L HEPES, pH 8.0, 2 mol/L NaCl, and 0.01% Triton X-100 at 27°C. CatG (EMD) activity was measured using Suc-Ala-Ala-Pro-Phe-AMC (MP Biomedicals) in assay buffer consisting of 50 mmol/L NaOAc, pH 5.5, 2 mmol/L EDTA, and 1 mmol/L dithiothreitol (DTT) at 30°C. CatA (R&D Systems) activity was measured using MCA-Arg-Pro-Pro-Gly-Phe-Ser-Ala-Phe-Lys(Dnp) in assay buffer consisting of 50 mmol/L MES, pH 5.5, and 5 mmol/L DTT at 27°C. DPPII (R&D Systems, Inc.) activity was measured using Suc-Lys-Pro-AMC (MP Biomedicals) in assay buffer consisting of 25 mmol/L MES, pH 6.0, at 27°C. IC_{50} (50% inhibitory concentration) values were determined on the basis of the reaction velocity measured between 60 and 75 minutes by using GraphPad Prism 4.01. HtrA2/Omi (R&D Systems) activity was measured in a gel-based assay using β-casein (Sigma-Aldrich Corp.) as a substrate as described by the manufacturer. The processed proteins were resolved by SDS-PAGE and detected by silver staining (Invitrogen).

Detection of protease activity in lysates

PBMC lysate IC_{50} determinations. A total of 2×10^6 to 3×10^6 cells were lysed per condition in 50 to 100 μL of lysis buffer [PBS with 1% Nonidet P40 (NP40)] for 1 hour on ice. Lysates were cleared by centrifugation and treated with inhibitor at various concentrations for 30 minutes, followed by 1-hour incubation with 10 μmol/L FP-biotin at room temperature (RT). SDS was added to a final concentration of 1% (5 μL in a 50 μL reaction volume) and the samples were boiled for 5 minutes. The SDS was diluted to 0.1% with PBS (V_F = 500 μL) and incubated with rotating overnight with 20 μL of prewashed Pierce Streptavidin UltraLink Resin (Thermo Scientific) at RT. FP-biotin–bound proteome resin was washed 3 times in lysis buffer, and after the final wash, any remaining liquid was extracted with a 30-gauge needle. The resin was resuspended in 10 μL PBS, 20 μL 4× SDS-PAGE loading dye (Bio-Rad), and 3 μL of 10× reducing agent (Bio-Rad). The FP-biotin–bound proteome was eluted by 3 cycles of 5 minutes boiling and vortexing. The eluate (10 μL) was loaded onto each lane for Western blot analysis. The signal was quantitated by densitometry using ImageJ software (http://rsbweb.nih.gov/ij/) and IC_{50} values were determined by GraphPad Prism 4.01. Antibodies used for Western blotting were mouse monoclonal anti-human CatA and anti-human chymase obtained from R&D Systems, rabbit polyclonal anti-human CatG and anti-human DPPII purchased from Abcam, and horseradish peroxidase–conjugated (HRP) secondary antibodies obtained from Jackson ImmunoResearch Laboratories, Inc. ImmunoPure Streptavidin resin and HRP–streptavidin overlay were purchased from Thermo Scientific.

Profiling tumor cell lines. Tumor cells (1.5×10^6–3×10^6 cells per condition) were lysed in lysis buffer for 30 minutes on ice and cleared by centrifugation. The lysates were then incubated with 10 μmol/L bortezomib or carfilzomib for 30 minutes at RT and then probed with 5 μmol/L of FP-biotin at RT for 1 hour. Proteins were separated by SDS-PAGE chromatography and FP-bound targets detected by Western blotting with HRP-conjugated streptavidin.

Ex vivo treatment of whole blood

Whole blood (10 mL) was treated with 100 nmol/L of bortezomib or carfilzomib for 40 minutes and transferred to BD Vacutainer cell preparation tubes (CPT; BD Biosciences) to isolate PBMCs. After centrifugation, PBMCs were collected, erythrocytes were removed by hypotonic lysis (BD PharmLyse; BD Biosciences), and the cells were lysed and cleared as described above. Cleared lysate was probed with 5 μmol/L of FP-biotin at RT for 1 hour. CatG was detected as described above.

Published OnlineFirst March 1, 2011; DOI: 10.1158/1078-0432.CCR-10-1950

Pharmacodynamics *in vivo*

Rats received intravenous bolus administration of bortezomib at 0.3 mg/kg and carfilzomib at 7 mg/kg. Fifteen minutes after dosing, animals were sacrificed by CO_2 narcosis, and blood and spleens were collected and processed as described previously (24). Proteasome CT-L activity was measured as described previously (24), and CatG activity in lysates from erythrocyte-depleted splenocytes was measured by FP-biotin probe binding as described above by using an anti-rodent CatG antibody (Santa Cruz Biotechnologies).

Whole blood (10 mL) was collected from consenting patients receiving 1.0 ($n = 1$), 1.3 ($n = 2$), or 1.6 mg/m^2 ($n = 1$) bortezomib into CPT to isolate PBMCs as described above. Proteasome and CatG activity was measured as described above. The study was approved by the independent cantonal Research Ethics Review Board and carried out in accordance with good clinical practice guidelines, the Declaration of Helsinki, and the applicable national law.

Western blotting for HtrA2 substrates

SH-SY5Y cells were seeded at 3×10^5 cells/mL and cultured for 2 days. The cells were then treated for 12 hours with carfilzomib or bortezomib (both at 100 nmol/L) and harvested for Western blotting analysis. Cell pellets were lysed in PBS + 1% NP40 + protease inhibitor cocktail (Roche Diagnostics) for 1 hour on ice and the lysates were cleared by centrifugation. Proteins were resolved by SDS-PAGE, transferred to nitrocellulose, and probed with antibodies for HtrA2, eIF4G1, and pyruvate dehydrogenase. All the antibodies were purchased from Abcam.

Statistical analysis

For comparisons of treatment groups, a 1-way ANOVA followed by Bonferroni post hoc analysis using GraphPad Prism (version 4.01) was done. Statistical significance was achieved when $P < 0.05$.

Results

Bortezomib induces neurite degeneration *in vitro* by a proteasome-independent mechanism

To investigate the role of proteasome inhibition in neurite degeneration, an *in vitro* assay was employed. This assay involved the differentiation of the human neuroblastoma cell line SH-SY5Y in the presence of retinoic acid and brain-derived neurotrophic factor, followed by exposure to proteasome inhibitors (22). Following treatment, cells were stained with Hoechst dye (blue) to detect nuclei and fluorescein isothiocyanate (FITC) anti–βIII-tubulin (green) to detect neurite outgrowth and analyzed using a high-content image analysis

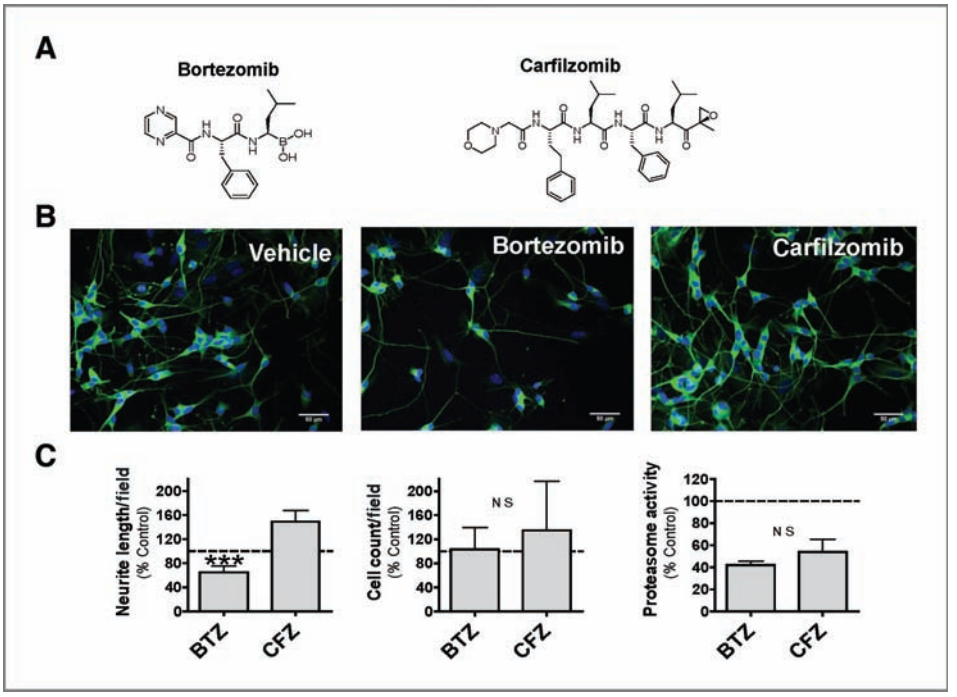

Figure 1. Bortezomib induces neurite degeneration *in vitro* by a proteasome-independent mechanism. A, chemical structures of bortezomib and carfilzomib. B, SH-SY5Y cells were differentiated, treated in triplicate for 24 hours with control (DMSO), 10 nmol/L bortezomib, or 10 nmol/L carfilzomib and stained with Hoechst nuclear stain (blue) to quantify cell number and neuronal-specific FITC–βIII-tubulin (green) to visualize neurite lengths. Representative fluorescent images (20×) for each condition are shown. C, quantitative analysis of cell count, neurite length (μm), and the ratio of average neurite length per field was done by using the fluorescent images and high-content image analysis software containing algorithms designed for morphologic segmentation and measurement. Twenty fields of view were analyzed per well. The experiment was done twice with similar results. Proteasome activity was measured by a fluorescent substrate (Suc-LLVY-AMC) assay. ***, $P < 0.05$ by 1-way ANOVA and Bonferroni post hoc testing. BTZ, bortezomib; CFZ, carfilzomib; NS, not significant.

Published OnlineFirst March 1, 2011; DOI: 10.1158/1078-0432.CCR-10-1950

Table 1. IC_{50} values of serine proteases in purified enzymes and PBMC lysates

		IC_{50} (μmol/L)			
		Carfilzomib		Bortezomib	
Target	P1 selectivity	Purified enzyme	PBMC lysate[a]	Purified enzyme	PBMC lysate[a]
CatA	F, Y, V, E	>10	>10	2.5 (1.6–4.1)	0.0047 (0.0022–0.0098)
CatG	L, F, H, Y, N, I, V	>10	>10	0.95 (0.77–1.2)	0.3 (0.12–0.76)
Chymase	F, Y	>10	>10	0.28 (0.26–0.31)	0.0016 (0.00071–0.0036)
DPPII	P, A, R	>10	>10	8.7 (5.6–14)	0.26 (0.17–0.4)
HtrA2/Omi	L, V	>10	N/A	0.003 (0.001–0.009)	N/A
Proteasome (LMP7)	L, F	0.025 (0.015–0.041)	0.022 (0.016–0.030)	0.031 (0.021–0.047)	0.00099 (0.00063–0.0016)

NOTE: 95% CIs are shown within parenthesis.

Abbreviation: N/A, not available.

[a]Lysate IC_{50} values were generated by using the ABP method except LMP7 activity which was measured by using a fluorogenic substrate assay.

software (Fig. 1B). Exposure of differentiated cells to 10 nmol/L bortezomib resulted in a 40% reduction in total and average cellular neurite lengths that was not a result of cell death (Fig. 1C). Exposure to an equimolar concentration of carfilzomib did not affect neurite length or cell viability in this system. Both agents resulted in equivalent levels of proteasome inhibition (~60%) following 1 hour of exposure (Fig. 1C). After 72 hours of drug exposure across a concentration range of 10 μmol/L to 1 nmol/L, both agents caused neurite loss that was associated with cell death (data not shown). Even with these longer exposures, bortezomib was 5.6- and 11-fold more potent than carfilzomib at inducing cell death and inhibiting neurite length, respectively. The observation that carfilzomib does not alter neurite morphology at noncytotoxic concentrations despite potent proteasome inhibition suggests that neurite degeneration induced by bortezomib is mediated by a mechanism that is independent of proteasome inhibition.

Bortezomib inhibits multiple serine proteases *in vitro*

Bortezomib has been shown to inhibit the serine proteases chymotrypsin, CatG, and chymase but not proteases with a preference for basic residues at P1, such as thrombin (19). We used a candidate approach to compare the activity of bortezomib and carfilzomib against a panel of 21 serine, cysteine, aspartyl, and metalloproteases (Supplementary Fig. S1). At 10 μmol/L, bortezomib inhibited serine proteases with a P1 selectivity of large hydrophobic or aromatic amino acids (chymotrypsin, CatG, and chymase) by 95% and elastase, rennin, and angiotensin-converting enzyme by 30% to 40%. On the other hand, carfilzomib displayed modest inhibition of chymotrypsin (~40%) but had minimal to no activity against the other 20 proteases. These data show that bortezomib has a broader off-target activity profile against nonproteasomal proteases than was previously considered.

To broadly profile the activity of bortezomib as an inhibitor of serine hydrolases, we utilized an ABP approach using a general serine hydrolase probe FP-biotin (refs. 19, 20; Supplementary Fig. S2). Lysates from 3 PBMC samples, an easily accessible primary human tissue that is a rich source of proteases (Supplementary Table S1), were exposed to both proteasome inhibitors prior to the addition of the FP-biotin probe. Isolated streptavidin-bound proteins were identified by liquid chromatography and tandem mass spectrometry (LC/MS-MS). As a validation of the method, we found that the broad-based protease inhibitors difluorophosphonate and diisocoumarin) resulted in the inhibition of several serine hydrolases (Supplementary Table S1). Further validating this approach, CatG inhibition by bortezomib was detected. By the ABP approach, we also detected inhibition of CatA and DPPII by bortezomib, 2 proteases that were not evaluated in the candidate screen (Supplementary Table S1). Carfilzomib did not result in significant inhibition of serine proteases in PBMC lysates as measured by ABP profiling.

We extended these findings by determining the relative potency of bortezomib by using fluorescent substrate assays on purified CatG, CatA, chymase, and DPPII. Bortezomib had varying potencies against these purified enzymes, with IC_{50} values ranging from 0.3 to 9 μmol/L (Table 1). To investigate whether the activity of the enzymes might differ in a complex cellular milieu, we determined the IC_{50} values by using the FP-biotin probe and a gel-based assay (Table 1 and Fig. 2A). In each case, bortezomib was more potent against serine proteases in cell lysates versus purified enzymes. For CatA and chymase, IC_{50} values were equivalent to those of the proteasome. Carfilzomib did not result in significant inhibition of these serine proteases in either assay system. These data show potent inhibition of several serine protease targets of bortezomib in physiologically relevant conditions.

Next, we utilized the FP-biotin probe to detect protease inhibition in 3 tumor cell lines. Lysates of HepG2

Published OnlineFirst March 1, 2011; DOI: 10.1158/1078-0432.CCR-10-1950

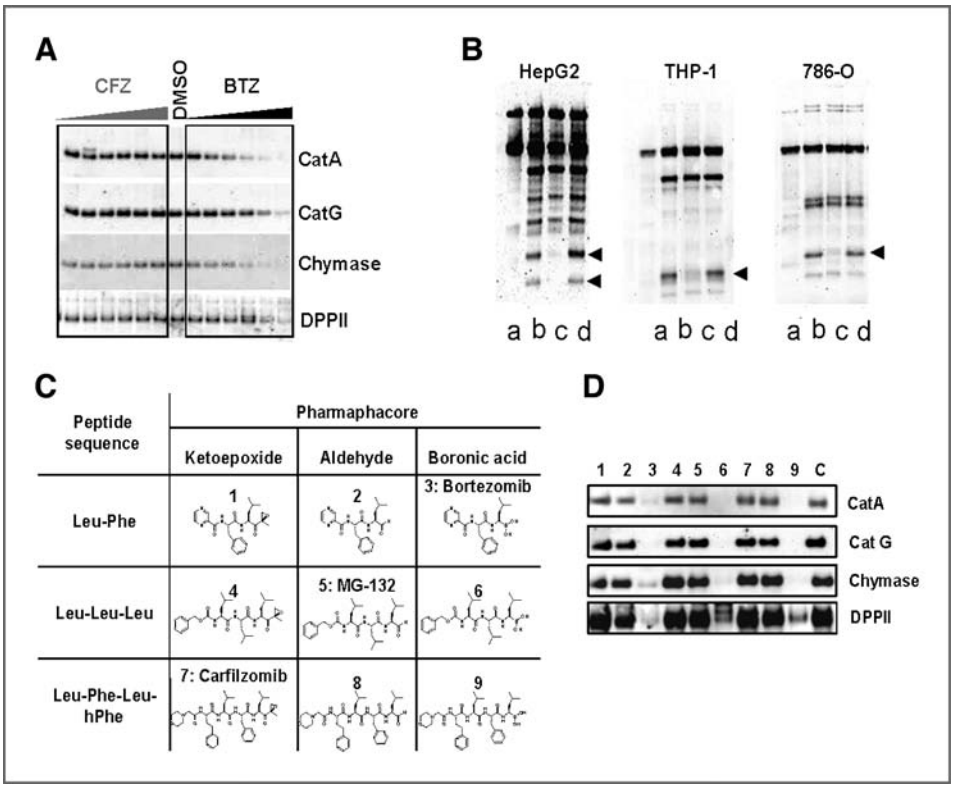

Figure 2. Peptide boronic acids are potent serine protease inhibitors. A, PBMC lysates were treated with carfilzomib (CFZ) or bortezomib (BTZ) at concentrations ranging from 0.1 nmol/L to 10 μmol/L followed by FP-biotin probe binding, SDS-PAGE, and Western blotting. Samples were probed with antibodies to CatA, CatG, chymase, and DPPII. A representative blot of 2 replicates is shown and IC_{50} values are presented in Table 1. B, lysates from HepG2, THP-1, and 786-O cells were heat-inactivated for a negative control (lane a), or treated with 1% DMSO (lane b), 10 μmol/L bortezomib (lane c), or 10 μmol/L carfilzomib (lane d). Lysates were treated with CFZ and BTZ as in A and blots were probed with streptavidin–HRP. Arrowheads indicate the FP-biotin reactive targets competed by BTZ. One of 2 representative experiments was carried out . C, structures of the epoxyketone, aldehyde, and boronic analogues of peptide epoxyketone inhibitors. BTZ (3), MG-132 (5), and CFZ (7) are indicated. D, PBMC lysates were treated with compounds 1 to 9 at 10 μmol/L and analyzed as described for A. C, DMSO control.

(liver adenocarcinoma), THP-1 (monocytic leukemia), and 786-O (renal adenocarcinoma) were exposed to bortezomib or carfilzomib. In all samples, we detected one or more FP-biotin–reactive protein species whose binding to FP-biotin could be blocked by prior exposure to 10 μmol/L bortezomib but was not affected by carfilzomib (Fig. 2B). We identified CatA as a bortezomib target in HepG2 lysates and CatG in THP-1 cells lysates (data not shown). Taken together, these data show a broad and variable profile of nonproteasomal targets for bortezomib.

Peptide boronic acids are potent serine protease inhibitors

Two possible explanations for the striking difference in serine protease inhibition between bortezomib and carfilzomib are the peptide length (dipeptide vs. tetrapeptide) and the reactive pharmacophore (boronate vs. epoxyketone). Indeed, peptide boronates have been described as potent serine protease inhibitors (25, 26). To address the roles of peptide length and pharmacophore on off-target activity, we generated a matrix of 9 compounds related to the peptide backbones of carfilzomib (hPhe-Leu-Phe-Leu), MG-132 (Leu-Leu-Leu), and bortezomib (Phe-Leu), in which each of the peptide backbones were synthesized with each of the 3 pharmacophores, epoxyketone, aldehyde, and boronate (Fig. 2C). PBMC lysates were exposed to each compound and probed with FP-biotin and Western blotting for 4 target proteases (CatG, CatA, DPPII, and chymase). Boronate-containing compounds, regardless of the peptide backbone, were potent inhibitors of serine proteases, whereas none of the epoxyketone containing inhibitors resulted in detectable inhibition (Fig. 2D). Aldehyde-based compounds were also unable to inhibit FP probe binding, further suggesting that serine protease inhibition is driven by the boronate pharmacophore. These data were further validated by fluorogenic substrate assays with CatG and the 3 warhead versions of Leu-Leu-Leu (compounds 4–6) in which only the boronic acid analogue (compound 6) was capable of inhibiting enzymatic activity ($IC_{50} = 78$ nmol/L).

Bortezomib inhibits serine proteases in intact cells and *in vivo*

Following exposure of intact PBMCs to bortezomib, we could detect CatG inhibition via ABP profiling, suggesting

Published OnlineFirst March 1, 2011; DOI: 10.1158/1078-0432.CCR-10-1950

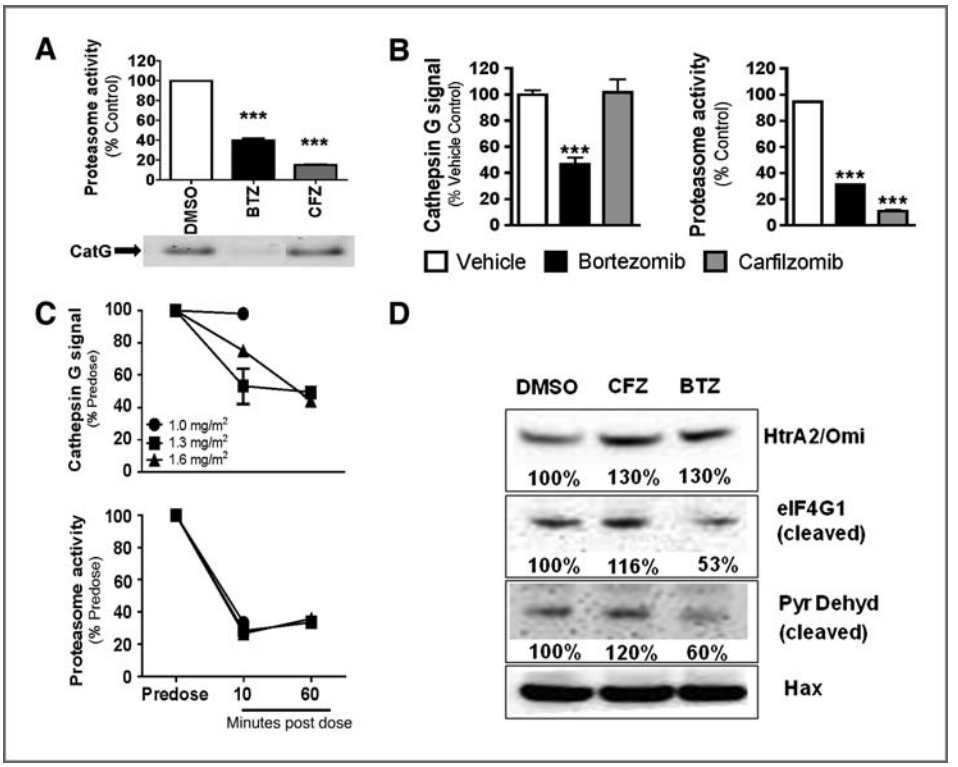

Figure 3. Bortezomib inhibits serine proteases *in vivo*. A, whole blood was incubated with bortezomib and carfilzomib for 40 minutes at 100 nmol/L and PBMCs were isolated. Lysates were exposed to FP-biotin and analyzed for the presence of CatG as described in Figure 2. Proteasome activity was measured as described in Figure 1. B, splenocytes were isolated from rats 15 minutes after receiving intravenous administration of vehicle, bortezomib (0.3 mg/kg), or carfilzomib (7 mg/kg). Lysates were probed with FP-biotin to detect CatG activity as described in Figure 2 or analyzed for proteasome activity as described in Figure 1. Values are presented as means (± SEM) relative to vehicle controls ($n = 3$ per group). The experiment was done twice with similar results. C, PBMCs were isolated from whole blood samples taken at predose and at 10 and 3,060 minutes postdose administration of 1.0, 1.3, or 1.6 mg/m^2 bortezomib on day 1 of cycle 1. All values are $n = 1$ except the 10-minute draw for the 1.3 mg/m^2 dose which represents an average (± SEM) of 2 patient samples. Lysates were probed for CatG and proteasome activity as described in B. D, undifferentiated SH-SY5Y cells were treated for 12 hours with DMSO, 100 nmol/L bortezomib, or 100 nmol/L carfilzomib. Lysates were analyzed for levels of HtrA2/Omi, eIF4G1, and pyruvate dehydrogenase and Hax, a protein required for HtrA2 activation was used as a control to show equal loading. Densitometry was carried out, and levels for each protein relative to DMSO-treated samples are indicated. Pyr Dehyd, pyruvate dehydrogenase.

that this approach could be applied to *in vivo* settings (data not shown). Subsequently, we incubated whole blood for 1 hour with 100 nmol/L of bortezomib, a concentration/exposure period maintained in patients receiving a dose of 1.3 mg/m^2 (19, 27, 28), and observed potent inhibition of CatG by ABP detection in isolated PBMCs. Carfilzomib, on the other hand, did not affect CatG activity despite equivalent levels of proteasome inhibition to bortezomib (Fig. 3A).

To determine whether bortezomib results in serine protease inhibition *in vivo*, bortezomib or carfilzomib were administered intravenously to rats and splenocytes were isolated 15 minutes after dosing and analyzed for inhibition of CatG and the proteasome. Bortezomib inhibited splenocyte CatG activity by 50% and proteasome activity by 70% (Fig. 3B). On the other hand, carfilzomib resulted in approximately 85% inhibition of the proteasome but no inhibition of CatG activity. Interestingly, when splenocytes were isolated 1 hour after administration of bortezomib, CatG activity had recovered to basal levels whereas proteasome inhibition remained at approximately 70% (data not shown).

Next, we investigated the inhibition of nonproteasomal proteases in PBMCs derived from myeloma patients treated with either agent. We found a time- and dose-dependent inhibition of CatG in patients receiving 1.0, 1.3, and 1.6 mg/m^2 bortezomib (Fig. 3C). One hour after administration of 1.6 mg/m^2, both CatG and proteasome CT-L and LMP2 activities were inhibited by 60% to 70% in PBMC samples (Fig. 3C and Supplementary Fig. S4). In the PBMC samples from patients treated with 20 mg/m^2 carfilzomib, no inhibition of CatG was detected in PBMCs of 2 solid tumor patients treated with 20 mg/m^2 bolus administration of carfilzomib despite proteasome inhibition of more than 75% (Supplementary Fig. S3). These findings show that nonproteasomal proteases are inhibited *in vivo* following administration of bortezomib.

By Western blot analysis, we could not detect expression of the bortezomib-targeted proteases identified in PBMCs (CatG, CatA, chymase, and DPPII) in SH-SY5Y cells

Published OnlineFirst March 1, 2011; DOI: 10.1158/1078-0432.CCR-10-1950

(data not shown). Furthermore, probing lysates from these cells with FP-biotin did not yield discernible proteins on streptavidin blots, indicating that target identification by LC/MS-MS would not be fruitful (data not shown). Therefore, we utilized a database mining approach to identify potential bortezomib targets that could be involved in the neurite degeneration in differentiated SH-SY5Y cells described previously (Fig. 1). MEROPS (http://merops.sanger.ac.uk/) is a comprehensive database of all known proteases and gene sequences predicted to be proteases. Of the 200 serine proteases in the database, 100 are annotated for a P1 preference. Of these, 14 proteases met our search criteria of having a P1 preference of Leu, Phe, or Tyr (Supplementary Table S2), with 5 of them already described above (CatG, CatA, chymase, and chymotrypsin B and C). We conducted literature searches on the remaining 9 candidates to determine whether a role in neurodegeneration or neuronal cell survival had been reported. One of these proteases, HtrA2/Omi, a stress-inducible mitochondrial protease involved in neuronal cell survival (29), was identified as a potential target. We utilized a gel-based assay to measure processing of the substrate β-casein by purified enzyme and found that bortezomib was an extremely potent inhibitor of HtrA2/Omi ($IC_{50} = 3$ nmol/L). We could detect HtrA2/Omi in SH-SY5Y cells and expression increased following a 12-hour exposure period to either proteasome inhibitor at 100 nmol/L (Fig. 3D). Interestingly, cleavage of the known substrates eIF4G1 and pyruvate dehydrogenase was inhibited in cells exposed to bortezomib but not carfilzomib (Fig. 3D). For both substrates, the amounts of cleavage products were higher in carfilzomib-treated cells than dimethyl sulfoxide (DMSO)-treated controls, correlating with the increase in expression of HtrA2/Omi. However, despite an increase in HtrA2 expression, there was no decrease in the cleavage of the 2 substrates in the bortezomib-treated cells, showing inhibition of the enzyme in these cells.

Discussion

PN has been described as the most important treatment-emergent adverse event associated with bortezomib therapy (8, 9, 19, 30). Recently published results with carfilzomib, a chemically distinct but equipotent proteasome inhibitor, suggest that PN is not a significant toxicity in treated MM patients (16, 17, 31, 32). Using an *in vitro* model of neurodegeneration, we found that bortezomib, but not carfilzomib, resulted in reduced neurite length and neuronal cell survival despite equivalent levels of proteasome inhibition with both agents. These findings mirror those obtained in animals receiving chronic administration of bortezomib in which rats and monkeys showed peripheral nerve degeneration and necrosis that manifested in behavioral changes such as tremors, reduced activity, and reduced sensory nerve conduction velocity (12, 33). In contrast, repeat dose administration of carfilzomib to rats and monkeys did not affect neurobehavior or result in histomorphologic changes to peripheral nerves (31). Although a randomized, comparative clinical trial with both agents will be required to provide definitive evidence, these findings suggest that PN is not a class effect of proteasome inhibitors, as has been proposed (34), but, rather, is a specific ADR of bortezomib.

We utilized a candidate screen approach to determine specific protease families and target profiles for bortezomib. From this, we utilized ABP profiling with a general serine hydrolase probe to survey primary cells for other nonproteasomal targets of bortezomib. When converted to a quantitative assay, we were able to show that bortezomib results in inhibition of multiple serine proteases with relative levels similar to the CT-L and LMP2 subunits of the proteasome. Importantly, we found that bortezomib administration to myeloma patients resulted in a potent and dose-dependent inhibition of one of these proteases (CatG). Future studies will explore the onset and recovery of CatG and other serine proteases in patient tissue samples following bortezomib exposure.

The use of the ABP approach to target profiling reveals several new and clinically relevant findings. By measuring off-target activity in physiologically relevant conditions (i.e., in cells and cell lysates), we found that bortezomib potently inhibited several serine proteases at clinically relevant concentrations. This suggests that the utilization of purified proteins may underestimate the potency of a drug against secondary targets. Furthermore, by using the ABP approach, we obtained an unbiased and broad survey for target profiling. The identification of DPPII, which has a strong preference for proline-containing dipeptides, as a target shows that bortezomib is a potent and promiscuous inhibitor of multiple classes of proteases. Finally, we show that secondary target inhibition can be monitored *in vivo* by the ABP approach. Inhibition of CatG in the spleen of bortezomib-treated rats shows tissue inhibition of nonproteasomal targets. Potent inhibition of CatG in PBMCs of patients receiving bortezomib is the first demonstration of the use of ABP profiling to monitor off-target activity in patients with an approved drug.

We also applied the ABP approach to show that serine protease inhibition is a generalized property of peptide boronates. When boronates are added to the tri- and tetrapeptide backbone of MG-132 and carfilzomib, respectively, the resulting compounds are potent serine protease inhibitors. Peptide epoxyketones, even the epoxyketone version of bortezomib, had no activity against serine proteases. Inhibition of DPPII by the tri- and tetrapeptide boronates suggests that the promiscuity of boronic acid–containing compounds may be broader than originally anticipated. However, we cannot rule out a role for the peptide backbone, as MG-132 could mediate potent inhibition of chymase as determined by the use of a fluorogenic substrate (data not shown). Although the ABP approach enables the detection of multiple targets in a physiologically relevant condition, such as primary cells, it is limited by the relative abundance of the probe to individual targets. This may explain

Published OnlineFirst March 1, 2011; DOI: 10.1158/1078-0432.CCR-10-1950

why chymase was not found in PBMCs via LC/MS-MS target identification but was detectable in Western blot analysis of PBMC lysates. Another limitation to the assay is the cellular source of targets. Indeed, we found distinct patterns of nonproteasomal target inhibition in individual tumor cell lines exposed to bortezomib. Further exploration with the ABP approach will involve different cell types and new active site probes. However, by utilizing the P1 preference for bortezomib against serine proteases we determined by using purified enzymes and ABP profiling, we were able to carry out database mining as a screen for other proteases that may be potential targets of bortezomib in cells but either lack affinity for the probe or are underexpressed in PBMCs. From this approach, we found that HtrA2/Omi, a serine protease with weak affinity for the FP-biotin probe (data not shown) and whose expression is induced following cellular stress, is potently inhibited by bortezomib.

HtrA2/Omi is expressed as mitochondrial and endoplasmic reticulum forms, each with distinct sets of substrates (35–37). Mitochondrial HtrA2/Omi has been shown to play a protective role in both *in vitro* and *in vivo* models of neurodegeneration and lymphocyte survival (29, 38–40). Following exposure to either bortezomib or carfilzomib, HtrA2/Omi expression increased in SH-SY5Y cells to levels similar to that reported for MG-132 (35), which may be the result of an unfolded protein response leading to oxidative stress. In these cells, processing of 2 substrates of HtrA2/Omi, eIF4G1, a translation factor, and pyruvate dehydrogenase, a Kreb cycle regulatory enzyme involved in generating oxidative species, are inhibited by bortezomib but not carfilzomib. Because both of these substrates have been implicated in neurodegenerative diseases (35, 41), inhibition of their processing may represent downstream mechanisms by which bortezomib alters neuronal cell function. Our data are consistent with a model in which bortezomib reduces neurite length by dual inhibition of the proteasome (resulting in oxidative and proteotoxic stress) and the neuronal prosurvival protease HtrA2/Omi.

In conclusion, we have utilized a multifaceted approach, including the first use of an ABP technique in clinical samples, to show that 2 structurally and mechanistically distinct proteasome inhibitors, bortezomib and carfilzomib, have dramatically different profiles for nonproteasomal targets *in vitro* and *in vivo*. Together with data from our *in vitro* model of neurite length inhibition, we propose that a specific ADR of bortezomib, PN, may be caused by distinct, off-target activities. Further exploration of the target profile for both agents by the approaches such as those described here is warranted.

Disclosure of Potential Conflicts of Interest

S. Arastu-Kapur, S.J. Lee, T. Muchamuel, and C.J. Kirk have ownership interest (including patents) in Onyx Pharmaceuticals, Inc.

Acknowledgments

The authors thank Dr. Susan Demo and Monette Aujay for assistance and the collaboration to obtain PBMCs from the bortezomib-treated patients, Dr. Matthew S. Bogyo and Andrew Guzetta (Stanford) for running mass spectrometry for nonproteasomal target identification, and Debbie Swinarski and Jing Jiang for their help with treating rats and harvesting samples. The authors also thank the Sarah Cannon Research Institute and University of Maryland for participating in the 007 solid tumor trial and collecting the carfilzomib patient samples.

Grant Support

C. Driessen, M. Kraus, and the Clinical Trials Unit at the Kantonsspital St. Gallen were supported by grants from the Swiss National Fonds (SNF), the Karl Danzer Stiftung, and the Wilhelm Sander Stiftung für Krebsforschung.

The costs of publication of this article were defrayed in part by the payment of page charges. This article must therefore be hereby marked *advertisement* in accordance with 18 U.S.C. Section 1734 solely to indicate this fact.

Received July 21, 2010; revised January 10, 2011; accepted February 14, 2011; published OnlineFirst March 1, 2011.

References

1. Peters JU, Schnider P, Mattei P, Kansy M. Pharmacological promiscuity: dependence on compound properties and target specificity in a set of recent Roche compounds. ChemMedChem 2009;4:680–6.
2. Funder JW. The off-target effects of torcetrapib. Endocrinology 2009;150:2024–6.
3. Ericson E, Gebbia M, Heisler LE, Wildenhain J, Tyers M, Giaever G, et al. Off-target effects of psychoactive drugs revealed by genome-wide assays in yeast. PLoS Genet 2008;4:e1000151.
4. Keiser MJ, Setola V, Irwin JJ, Laggner C, Abbas AI, Hufeisen SJ, et al. Predicting new molecular targets for known drugs. Nature 2009;462:175–81.
5. Orlowski RZ, Kuhn DJ. Proteasome inhibitors in cancer therapy: lessons from the first decade. Clin Cancer Res 2008;14:1649–57.
6. Adachi M, Zhang Y, Zhao X, Minami T, Kawamura R, Hinoda Y, et al. Synergistic effect of histone deacetylase inhibitors FK228 and m-carboxycinnamic acid bis-hydroxamide with proteasome inhibitors PSI and PS-341 against gastrointestinal adenocarcinoma cells. Clin Cancer Res 2004;10:3853–62.
7. Ciechanover A. Proteolysis: from the lysosome to ubiquitin and the proteasome. Nat Rev Mol Cell Biol 2005;6:79–87.
8. Richardson PG, Briemberg H, Jagannath S, Wen PY, Barlogie B, Berenson J, et al. Frequency, characteristics, and reversibility of peripheral neuropathy during treatment of advanced multiple myeloma with bortezomib. J Clin Oncol 2006;24:3113–20.
9. Cavaletti G, Jakubowiak AJ. Peripheral neuropathy during bortezomib treatment of multiple myeloma: a review of recent studies. Leuk Lymphoma 2010;51:1178–87.
10. Corso A, Mangiacavalli S, Varettoni M, Pascutto C, Zappasodi P, Lazzarino M. Bortezomib-induced peripheral neuropathy in multiple myeloma: a comparison between previously treated and untreated patients. Leuk Res 2010;34:471–4.
11. Orlowski RZ, Nagler A, Sonneveld P, Bladé J, Hajek R, Spencer A, et al. Randomized phase III study of pegylated liposomal doxorubicin plus bortezomib compared with bortezomib alone in relapsed or refractory multiple myeloma: combination therapy improves time to progression. J Clin Oncol 2007;25:3892–901.
12. Cavaletti G, Gilardini A, Canta A, Rigamonti L, Rodriguez-Menendez V, Ceresa C, et al. Bortezomib-induced peripheral neurotoxicity: a

Published OnlineFirst March 1, 2011; DOI: 10.1158/1078-0432.CCR-10-1950

neurophysiological and pathological study in the rat. Exp Neurol 2007;204:317–25.
13. Bennett MK, Kirk CJ. Development of proteasome inhibitors in oncology and autoimmune diseases. Curr Opin Drug Discov Devel 2008;11:616–25.
14. Dick LR, Fleming PE. Building on bortezomib: second-generation proteasome inhibitors as anti-cancer therapy. Drug Discov Today 2010;15:243–9.
15. O'Connor OA, Stewart AK, Vallone M, Molineaux CJ, Kunkel LA, Gerecitano JF, et al. A phase 1 dose escalation study of the safety and pharmacokinetics of the novel proteasome inhibitor carfilzomib (PR-171) in patients with hematologic malignancies. Clin Cancer Res 2009;15:7085–91.
16. Martin T, Singhal S, Vij R, Wang M, Stewart AK, Jagannath S, et al. Baseline peripheral neuropathy does not impact the efficacy and tolerability of the novel proteasome inhibitor carfilzomib (CFZ): results of a subset analysis of a phase 2 trial in patients with relapsed and refractory multiple myeloma (R/R MM). Blood 2010;116:3031.
17. Singhal S, Siegel DS, Martin T, Vij R, Wang M, Jakubowiak AJ, et al. Pooled safety analysis from phase (Ph) 1 and 2 studies of carfilzomib (CFZ) in patients with relapsed and/or refractory multiple myeloma (MM). Blood 2010;116:1954.
18. Kuhn DJ, Chen Q, Voorhees PM, Strader JS, Shenk KD, Sun CM, et al. Potent activity of carfilzomib, a novel, irreversible inhibitor of the ubiquitin-proteasome pathway, against preclinical models of multiple myeloma. Blood 2007;110:3281–90.
19. Adams J, Behnke M, Chen S, Cruickshank AA, Dick LR, Grenier L, et al. Potent and selective inhibitors of the proteasome: dipeptidyl boronic acids. Bioorg Med Chem Lett 1998;8:333–8.
20. Liu Y, Patricelli MP, Cravatt BF. Activity-based protein profiling: the serine hydrolases. Proc Natl Acad Sci U S A 1999;96:14694–9.
21. Eleuteri AM, Kohanski RA, Cardozo C, Orlowski M. Bovine spleen multicatalytic proteinase complex (proteasome). Replacement of X, Y, and Z subunits by LMP7, LMP2, and MECL1 and changes in properties and specificity. J Biol Chem 1997;272:11824–31.
22. Encinas M, Iglesias M, Liu Y, Wang H, Muhaisen A, Ceña V, et al. Sequential treatment of SH-SY5Y cells with retinoic acid and brain-derived neurotrophic factor gives rise to fully differentiated, neurotrophic factor-dependent, human neuron-like cells. J Neurochem 2000;75:991–1003.
23. Anderl JL, Redpath S, Ball AJ. A neuronal and astrocyte co-culture assay for high content analysis of neurotoxicity. J Vis Exp 2009;27:1173.
24. Demo SD, Kirk CJ, Aujay MA, Buchholz TJ, Dajee M, Ho MN, et al. Antitumor activity of PR-171, a novel irreversible inhibitor of the proteasome. Cancer Res 2007;67:6383–91.
25. Matteson DS. alpha-Amido boronic acids: a synthetic challenge and their properties as serine protease inhibitors. Med Res Rev 2008;28:233–46.
26. Kettner CA, Shenvi AB. Inhibition of the serine proteases leukocyte elastase, pancreatic elastase, cathepsin G, and chymotrypsin by peptide boronic acids. J Biol Chem 1984;259:15106–14.
27. Moreau P, Coiteux V, Hulin C, Leleu X, van de Velde H, Acharya M, et al. Prospective comparison of subcutaneous versus intravenous administration of bortezomib in patients with multiple myeloma. Haematologica 2008;93:1908–11.
28. Papandreou CN, Daliani DD, Nix D, Yang H, Madden T, Wang X, et al. Phase I trial of the proteasome inhibitor bortezomib in patients with advanced solid tumors with observations in androgen-independent prostate cancer. J Clin Oncol 2004;22:2108–21.
29. Martins LM, Morrison A, Klupsch K, Fedele V, Moisoi N, Teismann P, et al. Neuroprotective role of the Reaper-related serine protease HtrA2/Omi revealed by targeted deletion in mice. Mol Cell Biol 2004;24:9848–62.
30. Richardson PG. Towards a better understanding of treatment-related peripheral neuropathy in multiple myeloma. Lancet Oncol 2010;11:1014–6.
31. Vij R, Wang L, Orlowski RZ, Stewart AK, Jagganath S, Lonial S, et al. Carfilzomib (CFZ), a novel proteasome inhibitor for relapsed or refractory multiple myeloma, is associated with minimal peripheral neuropathic effects. Blood 2009;114:430.
32. Siegel DS, Martin T, Wang M, Vij R, Jakubowiak AJ, Jagganath S, et al. Results of PX-171–003-A1, an open-label, single-arm, phase 2 (Ph 2) study of carfilzomib (CFZ) in patients (pts) with relapsed and refractory multiple myeloma (MM). Blood 2009;116:985.
33. Bross PF, Kane R, Farrell AT, Abraham S, Benson K, Brower ME, et al. Approval summary for bortezomib for injection in the treatment of multiple myeloma. Clin Cancer Res 2004;10:3954–64.
34. Csizmadia V, Csizmadia E, Silverman L, Simpson C, Raczynski A, O'Brien L, et al. Effect of proteasome inhibitors with different chemical structures on the ubiquitin-proteasome system *in vitro*. Vet Pathol 2010;47:358–67.
35. Johnson F, Kaplitt MG. Novel mitochondrial substrates of omi indicate a new regulatory role in neurodegenerative disorders. PLoS One 2009;4:e7100.
36. Vande WL, Lamkanfi M, Vandenabeele P. The mitochondrial serine protease HtrA2/Omi: an overview. Cell Death Differ 2008;15:453–60.
37. Vande WL, Van DP, Lamkanfi M, Saelens X, Vandekerckhove J, Gevaert K, et al. Proteome-wide identification of HtrA2/Omi substrates. J Proteome Res 2007;6:1006–15.
38. Moisoi N, Klupsch K, Fedele V, East P, Sharma S, Renton A, et al. Mitochondrial dysfunction triggered by loss of HtrA2 results in the activation of a brain-specific transcriptional stress response. Cell Death Differ 2009;16:449–64.
39. Strauss KM, Martins LM, Plun-Favreau H, Marx FP, Kautzmann S, Berg D, et al. Loss of function mutations in the gene encoding Omi/HtrA2 in Parkinson's disease. Hum Mol Genet 2005;14:2099–111.
40. Chao JR, Parganas E, Boyd K, Hong CY, Opferman JT, Ihle JN. Hax1-mediated processing of HtrA2 by Parl allows survival of lymphocytes and neurons. Nature 2008;452:98–102.
41. Obeso JA, Rodriguez-Oroz MC, Goetz CG, Marin C, Kordower JH, Rodriguez M, et al. Missing pieces in the Parkinson's disease puzzle. Nat Med 2010;16:653–61.

AACR American Association for Cancer Research

Clinical Cancer Research

Nonproteasomal Targets of the Proteasome Inhibitors Bortezomib and Carfilzomib: a Link to Clinical Adverse Events

Shirin Arastu-Kapur, Janet L. Anderl, Marianne Kraus, et al.

Clin Cancer Res 2011;17:2734-2743. Published OnlineFirst March 1, 2011.